/5/ J. Merz, U. Witte
Dampferzeuger für gasgekühlte Reaktoren
Jahrbuch der Dampferzeugungstechnik Vulkan-Verlag, Essen,
3rd Edition 1976/77

/6/ Directory of Nuclear Reactors
International Atomic Energy Agency, Vienna

/7/ F. Dixon, H.K.Simons
The Central Electricity Generating Board's Nuclear Power Stations
A Review of the First 10 Years of Magnox Reactor Plant Performance and Reliability
J. Brit. Nucl. Energy Soc., 13, 1974, pp. 9-38

/8/ Informationsschrift AVR-Versuchskraftwerk, 1976

/9/ Arbeitsgemeinschaft Versuchsreaktor GmbH (AVR), Atom und Strom, Volume 25 (1979), No. 2

/10/ G. Bramblett, L. Meyer, W. Simon, F.E. Swart
Fort St. Vrain Status and Outlook
Tagungsbericht Jahrestagung Kerntechnik 1980, Berlin

/11/ Reactor Safety Study, an Assessment of Accident Risks in US Commercial Nuclear Power Plants, Appendix III und IV: Failure Data, US Nuclear Regulatory Commission PB-248204, 1975

/12/ P.D. Hedgecock, P. Patriarca
Materials Selection for Gas-Cooled Reactor Components, ANS Topical Meeting 'Gas-Cooled Reactors': HTGR and GCFBR, Gatlinburg, Tennessee, May 1974

/13/ Studie zur Ermittlung von Schadenswahrscheinlichkeiten für HTR-Dampferzeuger (on behalf of the Institute of Nuclear Safety Research at the KFA Jülich)
Sulzer, Winterthur, 1981.

DYNAMIC SIMULATION OF STEAM GENERATOR FAILURES

G. MEISTER
Institut für Nukleare Sicherheitsforschung,
Kernforschungsanlage Jülich GmbH,
Jülich, Federal Republic of Germany

Abstract

A computer program will be described which is capable to simulate severe transients in a gas heated steam generator. Such transients may arise in the safety analysis of accidents resulting from failures in the heat removal system of an HTGR power plant.

Important failure modes which have to be considered are ruptures of one or more steam generator tubes leading to water or steam ejection into the primary system or anomalous operating conditions which may cause damage due to excessive thermal stress. Examples are the complete dryout as a consequence of feedwater interrupt in connection with continuing gas heating and the reflooding of the secondary channel with cold feedwater after dryout.

The steam generator program which is capable to simulate accidents of this type is written as a module which can be implemented into a program system for the simulation of the total heat rejection system. It based on an advanced mathematical model for the two phase flow taking deviations from thermal equilibrium into account. Mass, energy and momentum balances for the primary and secondary fluid and the heat diffusion equations for the heat exchanging wall form a system of coupled differential equations which is solved numerically by an algorithm which is stiffly stable and suppresses effectively oscillations of numerical origin.

Results of the simulation of transients of the type mentioned above will be presented and discussed.

1. Introduction

The computer program SIKADE-2, which is introduced with this paper is part of a program system which has been developed for the dynamic simulation of accidents in HTGR plants. It simulates the transient reponse of typical HTGR steam generators on failures in the steam generator itself or from abnormal operating conditions which may come about as a consequence of failures

in the heat removal control system or from interventions by the plant operating personnel.
Abnormal conditions which have been taken into consideration until now are:

1. rupture of one or several steam generator tubes,
2. dry-out of a steam generator following a shut-off of the feed water supply and continuing heating on the primary side,
3. flooding of the steam generator after dry-out with cold feed water.

A rupture of steam generator tubes effects a water or steam ingress into the primary system of the reactor. Since steam generators in HTGR plants are normally operated at fairly high pressures on the secondary side (in the range of 200 bars) and since the gas pressure is much lower (in the range of 40 to 50 bars), high ejection rates result which increase the pressure in the primary system. For a long lasting water or steam ingress the pressure build-up may become large enough to endanger the confinement of the primary system. Water ingress accidents, therefore, have gained considerable attention in the past within the frame work of HTGR risk analysis.

Dry-out and re-flooding will cause severe thermal stresses which may result in a degradation of the steam generator performance. Time and space dependent temperature fields within the steam generator which are evaluated from a dynamic steam generator program may be used as boundary conditions for stress analysis.

2. Geometric Modelling

Most of the steam generators used in HTGR plants are designed at least in the economizer and evaporator part as a system of tube bundles with cross flow of the gas to the tubes. Preferred is an arrangement of the tubes in form of helix bundles. In the super-heating sections the same design mode is used in most cases but an arrangement of straight tubes with the gas flow parallel to the tubes has also been realized. Some steam generators have sections with downward flow and other sections with upward flow on the secondary side.

In order to meet the requirements of a variety of different designs the input specification of geometry is based on a scheme as sketched in Fig. 1. The steam generator is regarded as consisting of an abitrary number of sections with different geometry, different materials and different inclination against gravitational forces. All sections are connected in series with regard to flow on both sides. The flow direction in the primary and secondary channel may be opposite as shown in Fig. 1 but parallel flow is also admitted. More complicated cross connections of flow on the primary side between different sections cannot be treated with the present status of program development. Fluid ducts which are thermally isolated may also be specified in the same manner with the heat exchanging area set equal to zero.

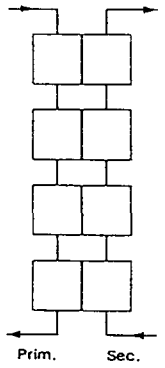

Fig. 1: Geometric Model of the Steam Generator design.

3. Mathematical Modelling

The equations governing the behaviour of the steam generator are basicly partial differential equations with time and space vectors as independent variables. The fluids are modelled by a set of equations representing mass-, energy- and momentum conservation. The heat transport within the walls of the tubes is described by a two-dimensional heat diffusion equation which takes the radial and axial heat diffusion into account. The coupling to the primary gas flow and the secondary two-phase flow is achieved by heat transfer correlations which, in the latter case, vary according to the local flow regime.

The two-phase flow in the secondary channel is governed by six coupled partial differential equations representing mass-, energy and momentum conservation for the two phases. Every pair of these equations is coupled by interphase transfer coefficients for mass, energy and monentum. Since mass, energy or momentum lost by one phase is gained by the other one these coefficients have the same absolute value but different sign in every pair of equations. The sum of any pair of equations, therefore, does not contain these exchange coefficients, because they cancel each other. The equations obtained in this manner are denoted as "mixture equations". The original system of equations and the system of the three mixture equations, each supplemented by one of the corresponding equations for one of the two phases is mathematically equivalent.

The complete system of equations has been formulated and discussed in several articles /1,2,3,4/. It appears to be the most advanced approach but it is not capable to predict the radial flow distribution in the different flow regimes without additional correlations.

The SIKADE-program is based on a simplified approach which is obtained if the complete system of equations is reduced to four equations. The energy transfer between the two phases is supposed to be given by the interphase mass transfer times the local difference of steam and liquid enthalpy. Since the mass transfer rate is a quantity appearing in the phase continuity equations either one of the energy equations or one of the continuity equations can be eliminated by substitution. The original set of two continuity and two energy equations is thus reduced either to one (mixture) continuity equation and two energy equations or two continuity equations and one mixture energy equation. The latter version has been selected for modelling in this program.

We note that thermal equilibrium is not yet assumed by implication. It would have to be assumed if the system of three equations is further reduced to two mixture equations only. Thermal equilibrium is not presupposed in the model underlying the program from reasons which will be discussed later.

The two momentum equations are replaced by the mixture equation only, supplemented by empirical correlations for two-phase friction and steam slip. Slip and frictional pressure gradients would come out as a result if the two momentum equations are used but the present knowledge about interphase momentum exchange in the different flow regimes seems to the author to be not more reliable than the friction and slip correlations available from literature.

The program is based on a one-dimensional approach in space for both fluid channels. This is certainly adequate for two-phase flow inside of tubes with small diameter since correlations are available which take radial distributions of fluid density and mass flow density properly into account. For the primary gasflow channel, however, this assumption implicates that the same axial distribution of gas temperature is assumed for all parallel tubes of a bundle.

The system of conservation equations has to be supplemented by a set of "constitutive" equations which define the pressure and temperature dependence of the thermodynamical properties of the

fluid. For water and steam these quantities are evaluated by subroutines which are based on IFC-formulations /17/.

Correlations for such quantities as heat transfer coefficients steam slip, friction coefficients, criteria for the incipience of boiling or for departure from nucleate boiling are included into the program as subroutines. Thus, correlations can easily be exchanged without interference to the mainstream of the program if, for instance, they should be replaced to meet a more recent state of knowledge.

For numerical integration each section of the steam generator is subdivided into an arbitrary number of discretization volumes. The dimensions of these volumes are given by the appropiate free flow area and an incremental height obtained from the total length of the section divided by the number of subdivisions. The original set of partial differential equations is then transformed to a system of coupled ordinary differential equations by applying Gauss' integral theorem to each volume. This type of generating difference equations is known as finite volume method.

Let V_n be a finite volume with its center at the axial coordinate z_n which has common interfaces with neighbouring volumes V_{n-1} and V_{n+1} at $z = z_{n-1/2}$ and $z = z_{n+1/2}$ respectively (see Fig. 2).

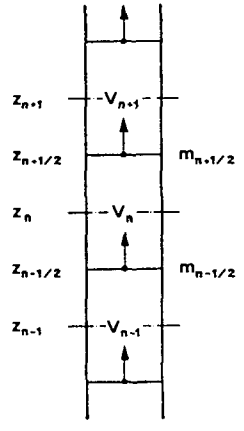

Fig. 2: Finite Volume Differencing of the Flow Channel

Then the integration of the mixture continuity equation

$$\frac{\partial \rho}{\partial t} + \frac{\partial m}{\partial z} = 0 \quad , \qquad (1)$$

yields the following ordinary differential equation

$$\frac{d M_n}{d t} = w_{n-1/2} - w_{n+1/2} \quad , \qquad (2)$$

where m is the mass flow density and M_n the total mass inventory of volume V_n. $w_{n-1/2} = A\, m_{n-1/2}$ and $w_{n+1/2} = A\, m_{n+1/2}$ are the mass flows at the two interfaces of the volume. The mass inventory is defined by $M_n = V_n \rho_n$ where ρ_n is an average value of the mixture density within the volume. Expressed in terms of water and steam density ρ_n is given by

$$\rho_n = \rho_{wn} (1 - \alpha) + \rho_{sn} \alpha \quad , \qquad (3)$$

where ρ_w and ρ_s are averages of the water and steam density respectively and α the volummetric steam fraction in the volume V_n. The mass flows appearing in equation (2) are evaluated by means of the momentum equation.

An analogous transformation of the mixture energy equation yields the following differential equation

$$\frac{d U_n}{d t} = H_{n-1/2} - H_{n+1/2} + J_{n-1/2} - J_{n+1/2} + Q_n \quad , \qquad (4)$$

where U_n is the total energy inventory of the volume, $H_{n-1/2}$ and $H_{n+1/2}$ are enthalpy fluxes while $J_{n-1/2}$ and $J_{n+1/2}$ are kinetic energy fluxes at the interfaces to the neighbouring volumes. Q_n is the total heat flux into the volume. The enthalpy flux is defined by $H = w\, h$ where h is the enthalpy density at the interface. Upwind differencing is used for sake of numerical stability, i.e. the enthalpy associated to each interface is set equal to the average enthalpy density in the upstream volume.

The energy inventory is given by

$$U_n = V_n (\rho_{wn} (1-\alpha) h_{wn} + \rho_{sn} \alpha h_{sn} + E_n) - V_n P_n \quad , \quad (5)$$

where h_w and h_s are average values of the water and steam enthalpy respectively, E_n is the average value of the kinetic energy density and P_n the average pressure within V_n.

Kinetic energy terms are included in the modelling of this program. Their contribution is normally small but may become significant if, for instance, a tube rupture leads to large flow rates.

The mixture momentum equation can be written as a partial differential equation in the form

$$\frac{\partial m}{\partial t} + \frac{\partial}{\partial z} (m\ v) = - \frac{\partial p}{\partial z} - g \cos\theta \cdot \rho - F \quad , \quad (7)$$

where m is the mass flow density of the mixture (averaged over the tube cross section). (m v) denotes the two-phase momentum flux density which, in general, is composed of a water and a steam contribution in the following manner

$$(m\ v) = m_w v_w + m_s v_s \quad , \quad (8)$$

v_w and v_s are water and steam velocities respectively. The second term on the right side of Eqn. (7) is the gravitational pressure gradient and F the friction pressure gradient which may be written in the form

$$F = \frac{1}{2} \frac{c_{tp}}{d_H} \frac{1}{\rho} |m|\ m \quad , \quad (9)$$

where c_{tp} is a two-phase friction coefficient.

Integrating equation (7) over a finite volume V_k of the flow channel yields

$$V_k \frac{d\bar{m}_k}{dt} = A\ (\langle m\ v\rangle_{k-1/2} - \langle m\ v\rangle_{k+1/2}) + A\ (P_{k-1/2} - P_{k+1/2}) - V_k\, g \cos\theta \cdot \rho_k - V_k \bar{F}_k \quad , \quad (10)$$

In this equation $\bar{m}_k$ denotes an average value of the mass flow density within the volume V_k, $\langle m\ v\rangle_{k-1/2}$, $\langle m\ v\rangle_{k+1/2}$ are momentum fluxes, and $P_{k-1/2}$, $P_{k+1/2}$ pressures on the interfaces of the volume which it has common with neighbouring volumes.

Since the average value of the mass flow density appearing on the left side of equation (10) has to be associated to a mass flow value at a volume interface in the corresponding equation for mass or energy conservation the finite volume grid used for the momentum equation (10) must be staggered with regard to the grid used for the continuity and energy equation.

The gradient of momentum flux is relatively small compared with other terms on the right side of equation (10) if the flow is in a single phase region without phase change. In the evaporation region, however, it forms the dominant contribution to the total pressure gradient.

Numerical experiments with different algorithms for the simulation of compressible fluid flow by C.W. Hirt /4/ have shown that the momentum convection may be a source of numerical instability leading to oscillations of the solution of the system of finite difference equations which do not correspond to oscillatory solutions of the system of the exact differential equations. The method of donor cell differencing which is recommended in ref. /4/ to suppress this effect, therefore, has been used in the formulation of the momentum difference equations in this program.

The correctness of the evaluated pressure distribution along the secondary flow channel has considerable influence on the results of a transient simulation of the two-phase flow. This results mainly from a feedback of the momentum equation to the

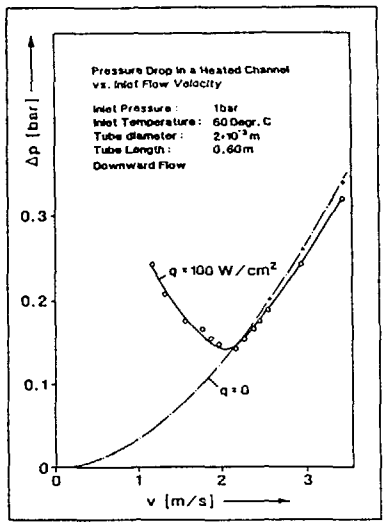

Fig. 3: Pressure Loss in a Heated Channel vs. Inlet Velocity

energy equation via the pressure dependence of the saturation temperature.

An essential contribution to the total pressure drop in the secondary flow channel may come from the region of subcooled boiling where a considerable fraction of steam may be present in spite of the presence of subcooled water. Fig. 3 shows measured total pressure losses in an electrically heated tube as a function of inlet water flow velocity /5/. For comparison the pressure loss in the unheated tube is also shown. The pressure loss characteristics of a heated channel with subcooled boiling flow is well demonstrated in this figure. The abnormal pressure drop behaviour at moderate and low inlet flows is known to be the origin of the parallel channel ('Ledinegg')-instability. A theoretical evaluation of the flow conditions in this experiment reveals that the assumption of thermal equilibrium would predict no steam generation at all in this case. Realistic modelling, however, shows that the steam fraction is considerable in the mass flow region where the pressure drop has its minimum and that the momentum flux contribution is dominant there.

In the subcooled region vapor bubbles are generated in the superheated water layer adjacent to the wall. If the bubbles grow beyond this layer or detach from the wall, they recondense within the subcooled bulk flow. The finite steam content results from the continuous generation and the finite lifetime of the vapor bubbles.

In order to take this effect into account the second continuity equation for the vapor phase is used to implement a vapor bubble generation and recondensation model into the two-phase flow model. The vapor continuity equation in its finite volume form may be written as

$$\frac{d M_{sn}}{d t} = w_{sn-1/2} - w_{sn+1/2} + V_n \Gamma_{svn} + S_n \Gamma_{ssn} \quad , \quad (11)$$

where Γ_{sv} is the volume steam generation rate and Γ_{ss} the surface generation rate. M_{sn} is the vapor inventory in the volume V_n. The surface generation rate may be expressed in the form

$$\Gamma_{ss} = q_L / h_{ev} \quad , \quad (12)$$

where q_L is that fraction of the total heat flux density which is consumed for vapor generation instead for convective heat transfer immediately to the water. The volume rate Γ_{sv} is negative due to vapor condensation and may be written in the form

$$\Gamma_{sv} = - \frac{1}{\tau} \alpha \rho_s \quad , \quad (13)$$

where τ is an effective vapor bubble lifetime. The lifetime depends on the local bulk fluid subcooling and, beside other quantities, on the local mass flow density. A theory of bubble lifetime has been developed and compared with measurements in ref. /6/. The latent heat flux density q_L is assumed to be given by the excess heat flux beyond the pure convective heat flux in the region of partial and fully developed nucleate boiling shown as a hatched area in Fig. 4.

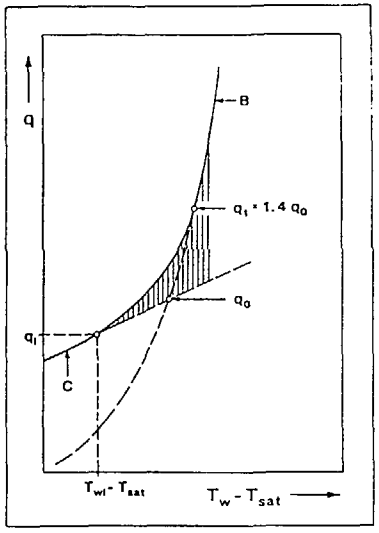

Fig. 4: Heat Flux as a Function of Wall Temperature for Partial and Fully Developed Nucleate Boiling.
C: Curve of Convective Heat Transfer,
B: Curve of Fully Developed Boiling.
Hatched Area: Assumed Fraction of Heat Consumed for Vapor Bubble Generation.
q_i Heat Flux at Incipience of Boiling.

In the simulation example discussed in the next chapter the following empirical or semi-empirical two-phase correlations are used:

Two-phase phenomenon	author(s), reference
Single phase heat transfer in bended tubes	Pethukov, B.S. /8/ (1974)
Incipience of boiling	Davis, E.J., Anderson, G.H. /11/, (1966)
Fully developed boiling	Müller, F. /9/, (1967)
Partial boiling	Interpolation between the incipience of boiling and heat flux q_1 on the curve of fully developed boiling as shown in Fig. 4
Steam slip ratio	Marchaterre, J.F., Hoglund, B.M. /10/, (1962)
Steam quality at departure from nucleate boiling	Doroshuk, V.E., Levitan, L.L., Lantzman, F.P. /12/, (1975)
Critical heat flux high pressures (> 100 bar)	Peskov, O.L., Subbotin, V.I., Zenkevich, B.A., Sergeyev, N.D. /13/, (1961)
low pressures (< 100 bar)	Becker, K.H. /14/, (1965)
Post dry-out heat transfer	Groeneveld, D.C. /15/, (1973)

The gas flow in the primary channel is modelled in an analogous manner as the single phase steam flow on the secondary side, i.e. by a system of three conservation equations for mass, energy and momentum.

Numerical integration of the resulting system of differential equations is performed with the backward difference algorithm of second order accuracy /16/. The method is semi-implicit and, therefore, requires the solution of a large system of nonlinear difference equations in every time step. This is achieved by a combination of successive overrelaxation and Newton-Raphson iteration techniques.

For an adequate representation of a large steam generator an amount of 50 to 100 finite volumes should be specified. Since every volume is represented by eight differential equations (3 for the primary, 4 for the secondary flow and one for heat exchanging wall) a system with a total amount of 400 to 800 difference equations results. The computational effort required to solve this system is nevertheless economic compared with an explicit method because the BDF method allows relatively large time steps due to its stiff stability.

4. Demonstration example

The example which will be discussed below has been selected to demonstrate the response of the program to an event sequence which comprises an initial tube rupture followed by an interruption of the feedwater supply (causing a partial dry out) and a subsequent attempt to restart the steam generator operation.

The steam generator layout underlying the example resembles a typical HTGR unit with a power rating of 100 MW under normal operating conditions.

An arrangement of parallel tubes in form of helix bundles is assumed for the economizer, the evaporation and the superheating section. Downward flow is assumed on the secondary side and cross flow to tubes on the primary side.

In order to keep the "downhill" evaporation stable each tube is equipped at the feedwater entrance with an orifice acting as a choke valve. The collective feed water supply line has upward flow direction. The wall of this line is assumed to be thermally isolated at the outer surface.

Tube dimensions are chosen as follows:

tube outer diameter	2,50 cm
tube wall thickness	0,26 cm
number of parallel tubes	80
tube material	Incoloy 800
total heat exchanging area (primary)	1200 m^2

The transient starts from steady state conditions. Imposed initial conditions and same values characterizing the initial state are listed below.

Inlet gas temperature	650 degr.C
outlet gas temperature	250 degr.C
inlet feed water temperature	180 degr.C
outlet steam temperature	509 degr.C
primary mass flow	48.14 kg/s
secondary mass flow	40.00 kg/s
primary inlet pressure	40 bar
secondary inlet pressure	236 bar
secondary outlet pressure	200 bar
secondary pressure at fluid saturation	213 bar.

For the primary channel a free flow area of 1.6 m^2 is assumed. The primary heat transfer coefficient according the chosen bundle geometry is calculated from correlations recommended in ref. /18/.

The following sequence of imposed boundary conditions is used for the example:

Time (s)	
0	rupture of a tube at the outlet of the last superheater section,
10	reduction of feedwater massflow to zero within 3 sec.,
10	reduction of the primary massflow from 48.14 to 4.2 kg/s within 20 sec.,
60	restart with increase of the feedwater flow from zero to 22 kg/s within 10 sec.,
70	increase of the primary mass flow from 4.2 kg/s to 25 kg/s within 20 sec.

Fig. 5 shows the history of the total massflow of the two-phase mixture in that tube which is subject to rupture. The simulation shows a sharp peak of the mass flow which, initially, is concentrated to a small part of the tube near the rupture position. Critical flow conditions prevail for a rather short period of time only (about 0.7 s). Rapidly increasing frictional pressure losses decrease the pressure inside the tube in the neighbourhood of the open end in such a manner that the outflow becomes subcritical with a short delay. The disturbance of mass flow spreads with increasing time along the channel towards the inlet but remains limited to that region where steam is present.

Steam generation during the subsequent period with no feedwater supply tends to fill the heated part of the tube completely with vapour. Fig. 7 shows the progressive extension of the steam fraction inside the tube. The short region near the inlet which remains free from steam is the unheated feedwater supply line.

The secondary wall temperature is shown in Fig. 6. The temperature distribution experiences a temporary break down in the superheater region in the time interval from about 20 to 30 secs after initiation of the transient. This is a consequence of the temporary interruption of gas heating about 10 secs after the tube rupture.

The evaporation region is shifted against the outlet forcing the wall temperature down to values slightly above the local saturation temperature. Fig. 7 shows that the outlet steam fraction drops in the same time interval slightly below 1 which a means that, temporarily, wet steam appears at the open end of the broken tube.

Water pumped into the tube during the subsequent period of steam generator restart acts like a piston which pushes the steam content towards the end of the tube. The effect is counteracted to a certain degree by condensation of steam in the liquid/steam

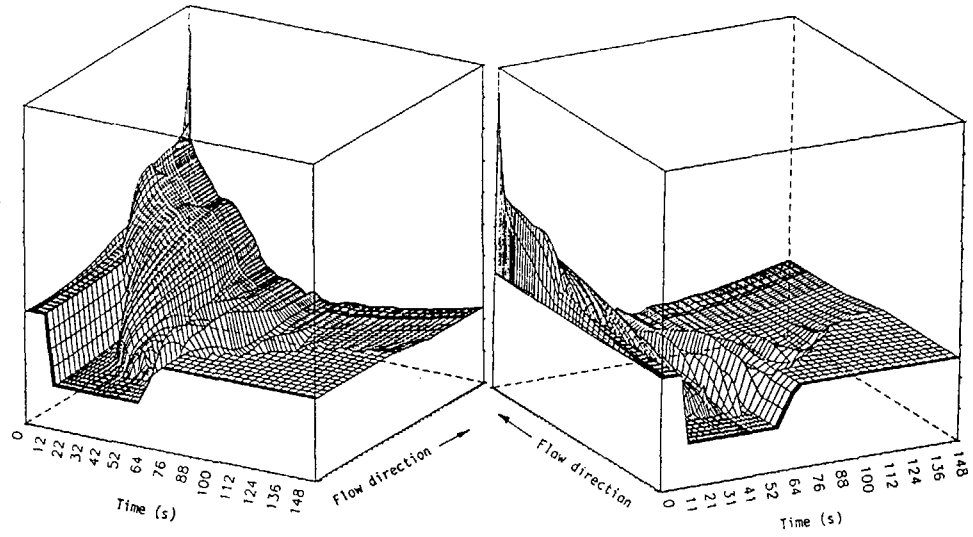

Fig. 5: Massflow distribution shown from two different view angles

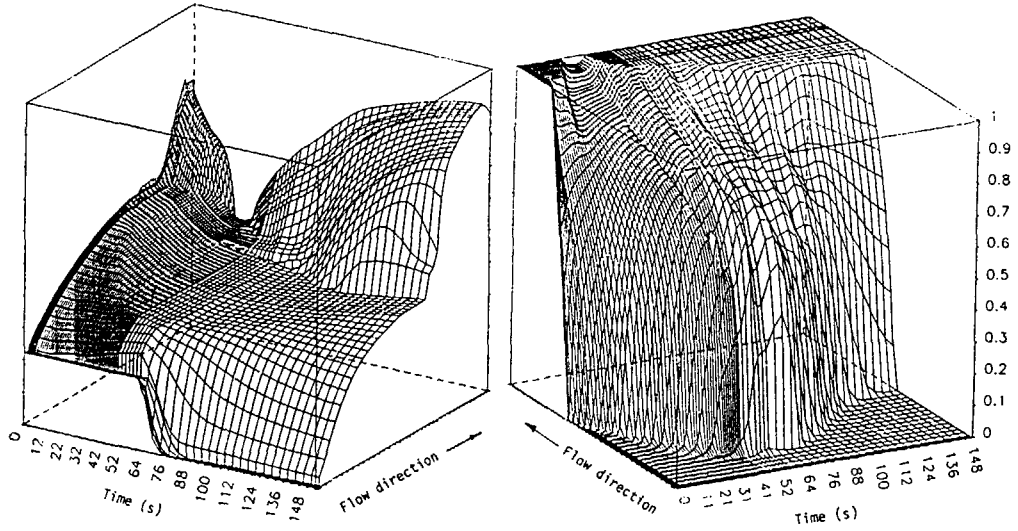

Fig. 6: Secondary wall temperature

Fig. 7: Steam volume fraction

contact region. The mass flow in this contact region is only moderately disturbed obviously because the steam can easily escape at the open end of the tube.

The time dependent pressure distribution inside the tube is shown in Fig. 9. The exit pressure is determined by the pressure boundary condition at the broken end. The inlet pressure, on the contrary, is treated as a dependent variable which is calculated from the prescribed inlet mass flow. The inlet pressure decreases during the initial period of time due to the depressurization at the exit and increases during the final period due to forcing the inlet massflow for restart of the steam generator.

Fig. 8 shows the time behaviour of the heat flux at the inner wall of the tube. The change from convective heat transfer to nucleate boiling can easily be identified during the initial time period up to 50 s from the higher level of heat flux density in the region of nucleate boiling. Short living peaks of the heat flux appear at the transition to departure from nucleate boiling. These peaks arise if a finite volume which was in the state of post dry-out heat transfer changes to nucleate boiling because the DNB boundary has changed its position in the channel. The transition to nucleate boiling causes a sudden release of part of the heat which was previously stored in the wall. It should be kept in mind, however, that the response of the program is not a quantitative simulation of the fluctuations which are normally present in this region. The program operates with heat transfer correlations in the post dry-out region which are known to be time averages of a strongly fluctuating process of dry-out and rewetting.

The temporary increase of heat flux near the inlet observed at the beginning of steam generator restart between 64 and 76 s results from a release of heat which was stored in the wall of the unheated feedwater supply line during the preceding transient.

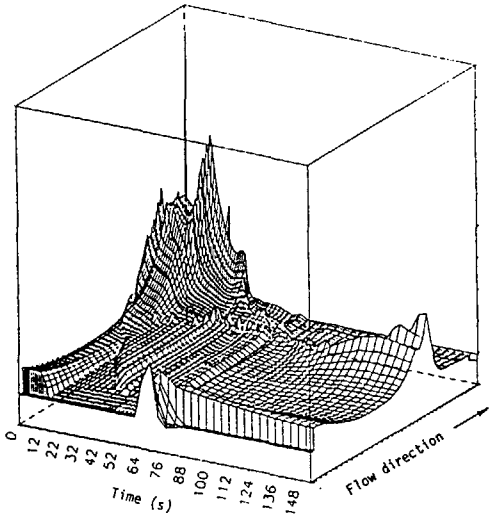

Fig. 8: Secondary heat flux density

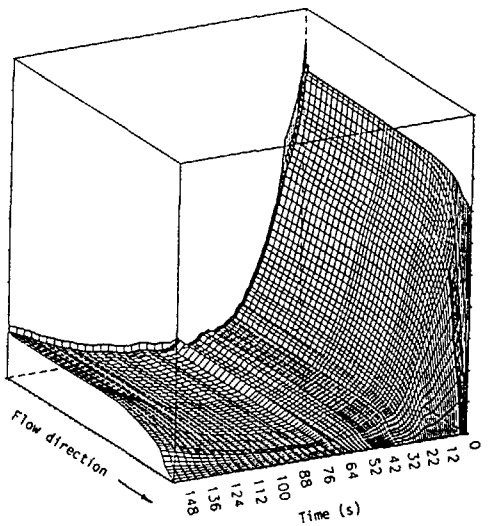

Fig. 9: Secondary pressure distribution

The extended region with high heat flux densities observed during the reflooding period results from an extension of the region of nucleate boiling due to the decreased pressure inside the tube which, meanwhile, has attained an average value of about 60 bar. The transition to post dry-out heat transfer is

more pronounced because the difference between nucleate boiling and post dry-out heat transfer at this pressure is larger than the difference at the rather high pressure level present at the beginning of the transient.

LIST OF SYMBOLS

A	free flow area
c_{tp}	two-phase friction coefficient
d_H	hydraulic diameter
E	kinetic energy density
F	friction pressure gradient
H	enthalpy flux
h	enthalpy
h_{ev}	vaporization enthalpy
J	kinetic energy flux
m	local mass flow density
$\bar{m}$	average mass flow density
M	total mass inventory of a volume V
M_w	water mass inventory of a volume V
M_s	steam mass inventory of a volume V
P	pressure
q_L	latent heat flux density
Q	heat flux
S	heat exchanging area
U	total energy inventory of a volume V
V	"finite" volume
v	fluid velocity
w	total mass flow
w_w	water mass flow
w_s	steam mass flow
z	axial coordinate
α	steam volume fraction
θ	inclination angle vs. horizontal direction
Γ_v	volume steam generation rate
Γ_s	surface steam generation rate
ρ	two-phase mixture density
ρ_w	water density
ρ_s	steam density
τ	vapour bubble lifetime

REFERENCES

/1/ Soo, S.L., Fluid Dynamics of Multiphase Systems. Blaisdell Publ. Comp. 1967

/2/ Mecredy, R.C., Hamilton, L.J., The Effects of Nonequilibrium Heat, Mass and Momentum Transfer on Two-Phase Sound Speed. Int. J. Heat Mass Transfer 15, (1972), pp. 61-72

/3/ Kolev, N.I., Homogene Zweiphasenströmung unter Bedingungen des vollständigen thermodynamischen Ungleichgewichts. Atomkernenergie-Kerntechnik 37, (1981), pp. 113-117

/4/ Ishii, M., Thermo-Fluid Dynamic Theory of Two-Phase Flow. Eyrolles 1975

/5/ Hirt, W.C., Heuristic Stability Theory for Finite Difference Equations. J. Comp. Phys. 2, (1968), pp. 339-355.

/6/ Meister, G., Vapor Bubble Growth and Recondensation in Subcooled Boiling Flow. Nucl. Engng. and Design 54, (1979), pp. 97-114.

/7/ Katscher, W., Anhalt, H., Zweiphasen-Druckverlustmessungen an durchströmten elektrisch beheizten Rohren. Zentralabteilung Forschungsreaktoren der KFA, 1971-1974.

/8/ Petukhov, B.S., Turbulent Heat Transfer in Tubes with Variable Fluid Properties. Article in "Heat Exchangers, Design and Theory Sourcebook", Afgan, N.H., E.U. Schlünder Eds. (1974)

/9/ Müller, F., Wärmeübergang bei der Verdampfung unter hohen Drücken. VDI-Forschungsheft 522 (1967)

/10/ Marchaterre, J.F., Hoglund, B.M., Correlation for Two-Phase Flow. Nucleonics 20, (1962), p. 142.

/11/ Davis, E.J., Anderson, G.H., The Incipience of Nucleate Boiling in Forced Convection Flow. A.I.Ch.E. Journ. 12, (1966), pp. 774-780.

/12/ Doroshuk, V.E., Levitan, L.L., Lantzmann, F.P., Investigations into Burnout in Uniformly Heated Tubes. ASME paper 75-WA/HT-22 (1975).

/13/ Peskov, O.L., Subbotin, V.I., Zenkevich, B.A., Sergeyev, N.D., Critical Thermal Fluxes during Forced Motion of Steam-Water, Water Mixture in Pipe, Article in "Problems of Heat Transfer and Hydraulics of Two-Phase Media" Kutateladze Ed. 1961. Transl. US Department of Commerce FTD-MT- 64-271

/14/ Becker, K.M., An Analytical and Experimental Study of Burnout Conditions in Vertical Round Ducts. AE-178 (1965).

/15/ Groeneveld, D.C., Post Dryout Heat Transfer at Reactor Operating Conditions. AECL-4513 Nat. Topical Meeting on Water Reactor Safety, Salt Lake City, 1973.

/16/ Lapidus, L., Seinfeld, J.H., Numerical Solution of Ordinary Differential Equations. Academic Press 1971.

/17/ VDI-Wasserdampftafeln. Springer-Verlag 1968.

/18/ Gnielinski, V., Wärmeübergang bei Queranströmung durch einzelne Rohrreihen und Rohrbündel VDI-Wärmeatlas, Chapter Ge and Gf (1977)